Influence of carrier localization at the core/shell interface on the temperature dependence of the Stokes shift and the photoluminescence decay time in CdTe/CdS type-II quantum dots

Taichi Watanabe, Kohji Takahashi, Kunio Shimura, and DaeGwi Kim*
Department of Applied Physics, Osaka City University, Osaka 558-8585, Japan
(Received 20 March 2017; revised manuscript received 9 June 2017; published 18 July 2017)

We have systematically investigated the temperature dependence of absorption, photoluminescence (PL), and PL decay profiles in CdTe-core and CdTe/CdS type-II quantum dots (QDs). In CdTe/CdS QDs, Stokes shifts and PL decay time become larger with an increase in temperature above 120 K, while those in CdTe-core QDs are almost independent of temperature. The unusual temperature dependence of Stokes shifts and PL decay time in CdTe/CdS QDs is understood by considering carrier localization at the core/shell interface at low temperatures and thermal-energy-assisted detrapping from localized-exciton to type-II exciton states at higher temperatures. Furthermore, a phenomenological rate-equation model is developed to explain the experimentally observed temperature-dependent PL decay time.

DOI: 10.1103/PhysRevB.96.035305

I. INTRODUCTION

Semiconductor nanostructures such as quantum dots (QDs) [1,2], quantum wires [3,4], and quantum wells [5,6] have attracted considerable attention and have been extensively investigated because they exhibit size-dependent characteristic properties originating from the quantum-confinement effect (QCE). Of particular interest, in semiconductor QDs, electrons and holes are three-dimensionally confined and have no freedom of spatial motion.

Preparation techniques for QDs are classified into two types: one is self-assembled QDs grown using molecular-beam epitaxy, and the other is synthesis of colloidal QDs using chemical reactions in the solution process. Moreover, III-V semiconductors, such as InAs and GaAs [7,8], and II-VI semiconductors [9,10] have been the main target materials for self-assembled QDs. II-VI semiconductors, such as CdSe, CdTe, and CdS, have also served this role for colloidal QDs [11,12]. In recent years, QDs of various materials such as ZnSe [13,14], $CuInS_2$ [15,16], and ZnS-$CuInS_2$ alloys [17] have been successfully synthesized from the viewpoint of the preparation of environment-adaptive QDs, as well as applications to light-emitting devices [18,19], biomolecular imaging [20], and photovoltaics [21,22].

It is well known that the QCE strongly influences the photoluminescence (PL) properties of QDs. Moreover, QCE enhances the spin-exchange interaction, causing a large splitting energy between the spin-singlet and -triplet states [23,24]. The spin-triplet state can then give rise to the so-called dark-exciton state, which contributes significantly to PL processes in QDs.

Preparation of core/shell QDs is another important technique for controlling the QDs' PL properties. Core/shell QDs are divided into two categories based on their potential structures: type-I and type-II QDs. In type-I QDs, electrons and holes are confined to the same space in the core; however, in type-II QDs, they are spatially separated due to the type-II band alignment. For type-I QDs, core QDs are covered by the shell layer to improve PL efficiency, and wide-gap semiconductor ZnS is the most commonly used shell material [25–27]. The most popular type-I QDs are CdSe/ZnS-core/shell QDs, which have been a model material for QD studies so far [28,29]. In contrast, in type-II QDs, the spatial separation of photoexcited carriers would prolong PL decay time [30–35]. Furthermore, the decay time can be controlled by changing the shell-layer thickness. As typical examples of colloidal type-II QDs, CdTe/CdSe [30,33] and CdTe/CdS QDs [32,34,35] were successfully synthesized, and the control of PL decay time by adjusting the shell-layer thickness has been investigated. Furthermore, in Ref. [31], the authors reported single-exciton optical gain in CdS/ZnSe type-II QDs.

In type-II QDs, carrier transfer between the core and shell materials occurs through a hetero interface. Thus, carrier localization due to interface defects and/or band-bending effects influences PL dynamics. Since PL measurements at low temperatures are sensitive to defects or localized states, a study of the temperature dependence of PL spectra and PL dynamics, especially at low temperatures, is very important to understand the PL mechanism in type-II QDs. The contribution of localized states to PL processes at low temperatures will be reflected in the temperature dependence of the Stokes shift that is defined as the difference in energy between absorption and PL peaks. Thus, it is necessary to measure the temperature dependence of absorption and PL spectra in order to discuss the temperature-dependent Stokes shift. Furthermore, by studying the temperature dependence of PL dynamics as well, it is possible to clarify the influence of carrier localization on PL processes.

In this paper, we report on systematic studies of the temperature dependence of absorption and PL spectra as well as PL decay profiles to understand the PL mechanism in CdTe and CdTe/CdS QDs. Stokes shifts and PL decay times in CdTe/CdS QDs become larger with increased temperature, while those in CdTe QDs are almost independent of temperature. The observed temperature dependence of the Stokes shift and PL decay time in CdTe/CdS QDs is explained by considering both carrier localization at the core/shell interface at low temperatures and thermal detrapping from localized-exciton to type-II exciton states at higher temperatures. A simple rate-equation model is developed to discuss the obtained experimental results of CdTe/CdS QDs.

*tegi@a-phys.eng.osaka-cu.ac.jp

II. EXPERIMENT

CdTe-core and CdTe/CdS-core/shell QDs were prepared by a hydrothermal method following the procedure described in Ref. [35]. The mean diameter of the CdTe core is 3.5 nm and the shell thickness is 2.3 nm. Both the dispersion of the core size and the shell thickness are ∼8%. The QD solution was mixed with a polyvinyl alcohol (PVA) aqueous solution, and the mixed solution was spread on a glass substrate. Finally, the excess water was evaporated by heating at 80 °C for 2 h. This process yielded film samples, that is, CdTe QDs dispersed in PVA films, enabling us to investigate the temperature dependence of optical properties.

Absorption spectra were measured using a double-beam spectrometer with a resolution of 0.2 nm. For measurements of PL spectra and PL decay profiles, a laser diode (405 nm, Hamamatsu PLP10–040) with a pulse duration of 100 ps and a repetition frequency of 500 kHz was used as an excitation light. The emitted PL was analyzed with a single monochromator with a spectral resolution of 1 nm. The PL decay profiles were obtained by a time-correlated single-photon-counting method. The sample temperature was controlled using a closed-cycle helium-gas cryostat.

III. RESULTS AND DISCUSSION

Figure 1(a) shows the absorption and PL spectra of CdTe- and CdTe/CdS-QD solution samples. In the PL spectra, band-edge PL is dominant, and defect-related PL is negligibly weak. A well-defined 1*S* absorption peak is observed for the CdTe QDs, while the absorption spectrum of the CdTe/CdS QDs shows smearing of the 1*S* absorption peak. As discussed in previous reports [32,36], this smearing is a clear signature of a type-II transition characterized by reduced oscillator strength. Furthermore, in the absorption spectra of CdTe/CdS QDs, an additional absorption structure with stronger absorption intensity than the 1*S* transition is observed at ∼3 eV, which is a higher-energy region than the band-gap energy of ∼2.5 eV in a CdS bulk crystal. This transition originates from the higher excited states of electrons and holes spreading over entire QDs and leads to a greater oscillator strength due to a larger overlap integral of electron and hole wave functions.

Figure 1(b) shows the PL decay profiles of CdTe and CdTe/CdS QDs. It is obvious that the PL decay profile of the CdTe/CdS QDs is much longer than that of the CdTe QDs. As mentioned above, electrons and holes are spatially separated in the CdTe/CdS QDs due to the type-II band alignment. This spatial separation reduces the oscillator strength, thus causing the PL decay profile in the CdTe/CdS QDs to become longer compared to that in the CdTe QDs. To date, little attention has been paid to the temperature dependence of optical properties of CdTe/CdS QDs. In CdTe/CdS QDs, the electron transfers from the CdTe core to the CdS shell through the core/shell interface. In order to reveal the influence of electron localization at the interface on PL processes, it is necessary to conduct systematic studies of the temperature dependence of the Stokes shift and PL decay time in detail. Thus, we measured the temperature dependences of the absorption and PL spectra, as well as the PL decay profiles.

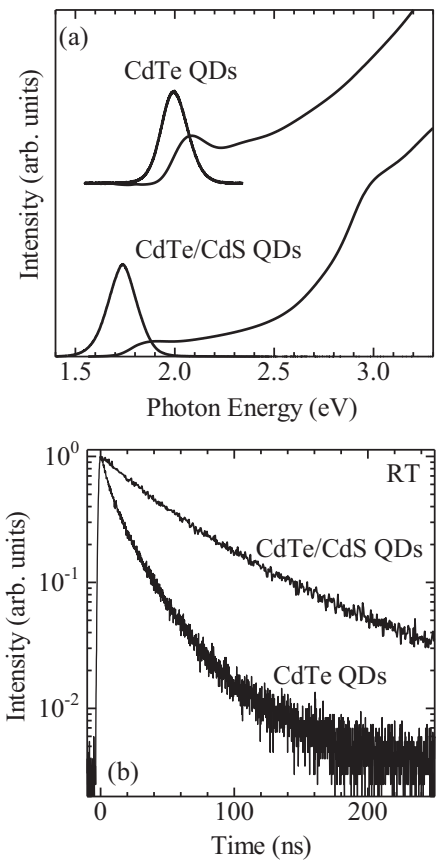

FIG. 1. (a) Absorption and PL spectra of CdTe and CdTe/CdS QD solution samples. (b) PL decay profiles of CdTe and CdTe/CdS QD solution samples.

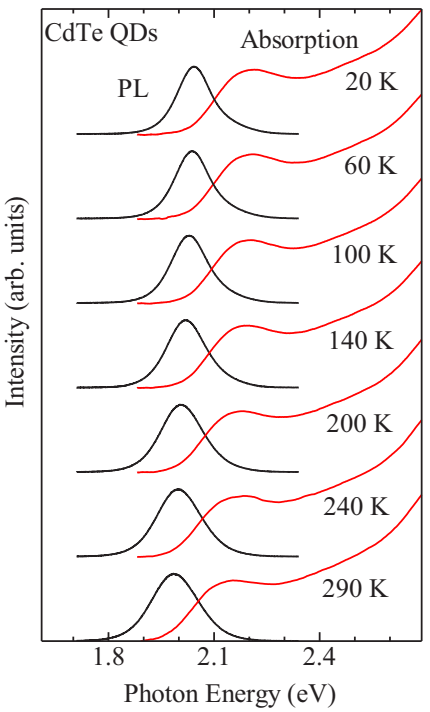

FIG. 2. Temperature dependence of absorption and PL spectra of CdTe QDs dispersed in PVA films.

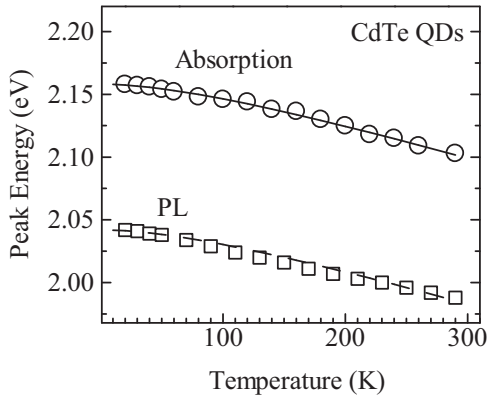

FIG. 3. Temperature dependence of absorption (open circles) and PL (open squares) peak energies in CdTe QDs. Solid and broken curves denote calculated results for the temperature dependence of the absorption and PL peak energies by using Varshni's law, respectively.

Figure 2 shows the temperature dependence of absorption and PL spectra of CdTe QDs. The absorption and PL peaks are redshifted with an increase in the temperature. The open circles and rectangles in Fig. 3 show the temperature dependence of the absorption and PL peak energies, respectively. The temperature dependence of the exciton energy usually reflects the temperature dependence of the band-gap energy [$E_g(T)$], and Varshni's empirical law well explains $E_g(T)$ in direct-gap semiconductors [37] as $E_g(T) = E_0 - \alpha T^2/(T+\beta)$, where E_0 is the band-gap energy at $T = 0$ K, α is the temperature coefficient, and β is a parameter related to the Debye temperature of the bulk crystal. The solid and broken curves denote calculated results for the temperature dependence of the absorption and PL energies, respectively, by using Varshni's law. In the calculation, the parameters of $\alpha = 3.0 \times 10^{-4}$ eV/K and $\beta = 185$ K in a CdTe bulk crystal [38,39] were used for both the absorption and PL energies. Thus, it is noted that the magnitude of the Stokes shift in the CdTe QDs is independent of temperature.

As shown in Fig. 2, only the band-edge PL is observed in the PL spectra at every temperature. The defect-related PL is negligibly weak even at a low temperature of 20 K. The intensity of the band-edge PL band at room temperature is ~76% of that at 20 K, demonstrating that the thermal-quenching effect is very small in the present CdTe QDs.

Figure 4 shows the temperature dependence of PL decay profiles. The observed profiles exhibit multiexponential decay as previously observed in colloidal QDs [40,41]. In Ref. [42], the authors analyzed PL decay profiles using a Kohlraush-Williams-Watts-type function. In order to discuss the temperature dependence of the decay time, we analyzed the PL decay profiles in a similar manner. The best fits were obtained with a combination of one stretched exponential and one monoexponential function: $A_1 \exp[-(t/\tau_1)^\beta] + A_2 \exp(-t/\tau_2)$. Here the parameters A_1 and A_2 represent the relative weights of the stretched-exponential and monoexponential components, respectively. For the stretched-exponential decay component, an average decay time of $\langle\tau_1\rangle = (\tau_1/\beta)\Gamma(1/\beta)$ can be obtained as in Ref. [42]. Since the intensity ratio of $\langle\tau_1\rangle$ over the τ_2 components is ~0.8 or greater for all decay profiles, we

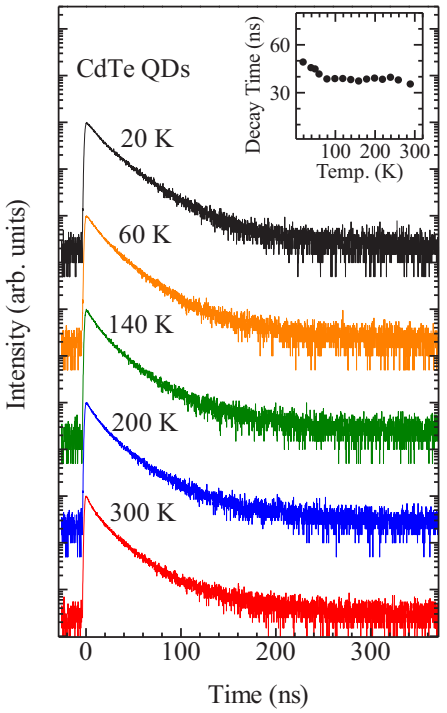

FIG. 4. PL decay profiles of CdTe QDs at 20, 60, 140, 200, and 300 K. The inset shows temperature dependence of PL decay time $\langle\tau_1\rangle$.

adopt the decay time of $\langle\tau_1\rangle$ as an intrinsic decay time. The dependence of $\langle\tau_1\rangle$ on temperature is plotted in the inset of Fig. 4. A noteworthy observation is that the temperature dependence of the PL decay profile was small; this was due to the feature that a splitting energy of ΔE between the bright- and dark-exciton states ($|\mathrm{Br}\rangle$ and $|\mathrm{Dx}\rangle$, respectively) in CdTe QDs is very small as compared with that in other II-VI semiconductor QDs such as CdSe and CdS QDs [24,43]. The previously reported values of ΔE range between 2 and 20 meV in CdSe and 5 and 60 meV in CdS QDs, which vary depending upon the QD size. In CdSe and CdSe/ZnS QDs, the PL decay profile becomes shorter with increased temperature. Moreover, the temperature dependence of the PL dynamics in CdSe and CdSe/ZnS QDs can be understood by a three-state model comprising a ground state and two excited states of $|\mathrm{Br}\rangle$ and $|\mathrm{Dx}\rangle$ [40,41]. With an increase in temperature, the thermal population of the higher-lying $|\mathrm{Br}\rangle$ becomes significant, and the decay time becomes shorter.

Conversely, since ΔE in the CdTe QDs is much smaller than that in the CdSe QDs (as has previously been investigated both theoretically [24] and experimentally [43]), the temperature dependence of $\langle\tau_1\rangle$ is small. The slight decrease in $\langle\tau_1\rangle$ below 60 K is considered to be due to the contribution of $|\mathrm{Dx}\rangle$, as previously reported in Ref. [43]. Furthermore, as mentioned above, the thermal-quenching effect in the present CdTe QDs is very small; thus, $\langle\tau_1\rangle$ was almost constant at a higher temperature than 70 K.

Figure 5 shows the temperature dependences of the absorption and PL spectra of CdTe/CdS QDs. We note that the PL intensity in these QDs at room temperature is ~80% of that at 20 K. Thus, as is the case for CdTe QDs, the thermal-quenching

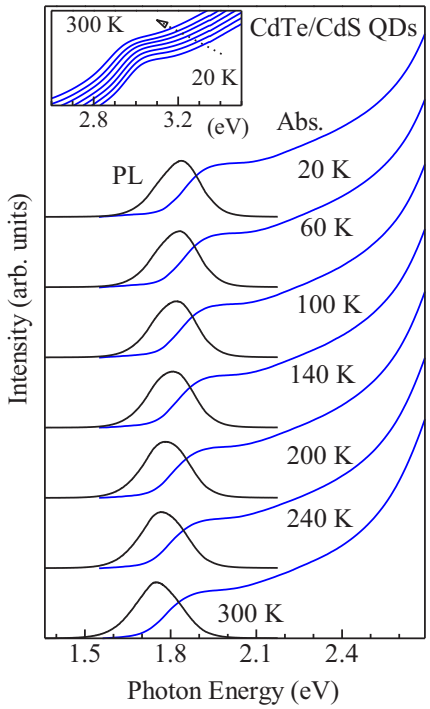

FIG. 5. Temperature dependence of absorption and PL spectra of CdTe/CdS QDs dispersed in PVA films. The inset shows enlarged absorption spectra in energy region of ∼3 eV.

effect is very small. The inset shows enlarged absorption spectra in the energy region of ∼3 eV, which corresponds to optical transition originating from the CdS shell. As was the case for CdTe QDs (Fig. 2), the absorption and PL peaks shift to the lower-energy side as temperature increases. In Fig. 6, the temperature dependences of absorption and PL energies are plotted by open circles and squares, respectively. The absorption spectra in CdTe/CdS QDs become broad compared with those in CdTe QDs due to a decrease in the oscillator strength originating from type-II transition. Thus, the absorption energy at every temperature was estimated from the energy minimum of the second-derivative spectrum.

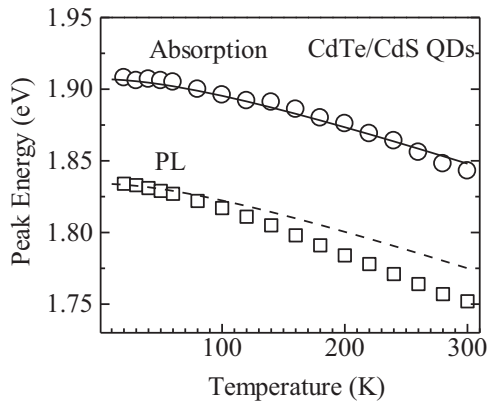

FIG. 6. Temperature dependence of absorption (open circles) and PL (open squares) peak energies in CdTe/CdS QDs. Solid and broken curves denote calculated results for the temperature dependence of the absorption and PL peak energies by using Varshni's law, respectively.

The solid and broken curves indicate calculated results for the temperature dependence of the absorption and PL energies by using Varshni's law. As was the case with CdTe QDs (Fig. 3), parameters of $\alpha = 3.0 \times 10^{-4}$ eV/K and $\beta = 185$ K in a CdTe bulk crystal were used for both the absorption and PL energies. The calculated result for the temperature dependence of the absorption energy quantitatively explains the experimental one. Conversely, for the temperature dependence of the PL energy, there is a discrepancy between the calculated result and the experimental one in the temperature region above 120 K, and it becomes larger with an increase in temperature. Thus, it is noted that the Stokes shift in CdTe/CdS QDs becomes larger with an increase in temperature in the temperature region above 120 K, while it is independent of temperature in CdTe QDs, as discussed in Fig. 3.

In order to discuss the temperature dependence of the Stokes shift, measurement of the temperature dependences of both the absorption and PL spectra is needed. However, there has been very little systematic study on this topic, while attention has been paid to the temperature dependences of absorption [44] or PL properties [41,45]. As an example of a report on the temperature dependence of the Stokes shift in a QD system, in Ref. [46] Liptay *et al.* investigated the temperature dependence of the Stokes shift in CdSe QDs. They observed the increase in the Stokes shift with temperature. As discussed above, in a QD system the QCE enhances the spin-exchange interaction, resulting in a large splitting energy between bright- and dark-exciton states. At low temperatures, a lower-lying dark exciton mainly contributes to the PL process, and the thermal population of a higher-lying bright exciton becomes larger with increase in temperature. As a consequence, the Stokes shift becomes smaller with temperature. The splitting energy in CdTe QDs is much smaller than that in CdSe QDs, as reported in Refs. [24,43]. Thus, the temperature dependence of the Stokes shift is supposed to be small. In fact, as discussed in Fig. 3, the Stokes shift is almost independent of temperature. Conversely, the Stokes shift in CdTe/CdS QDs becomes larger as temperature increases above 120 K. To our knowledge, no previous studies have reported such an unusual temperature dependence of the Stokes shift. We note that this finding was revealed by systematically measuring the temperature dependence of both absorption and PL spectra.

In order to investigate the origin of the anomalous temperature dependence of the Stokes shift in CdTe/CdS-core/shell QDs, we measured the temperature dependence of the PL dynamics. Figure 7 shows PL decay profiles of CdTe/CdS QDs at 20, 60, 140, 200, and 300 K. Since the observed profiles exhibit multiexponential decay, we analyzed PL decay profiles with a combination of one stretched-exponential function and one monoexponential function, as mentioned above. As in the case of the CdTe QDs (Fig. 4), because the relative intensity ratio of a stretched exponential component is ∼0.8 or greater for all the decay profiles, we adopt a decay time of $\langle\tau_1\rangle$ as an intrinsic decay time. The inset of Fig. 7 shows the temperature dependence of $\langle\tau_1\rangle$. $\langle\tau_1\rangle$ exhibits characteristic temperature dependence. In the temperature region between 20 and 120 K, $\langle\tau_1\rangle$ is almost constant. Then, at higher temperatures than 120 K, $\langle\tau_1\rangle$ becomes longer as temperature increases. Typically, the nonradiative-decay rate becomes larger with increasing temperature, resulting in decreases in

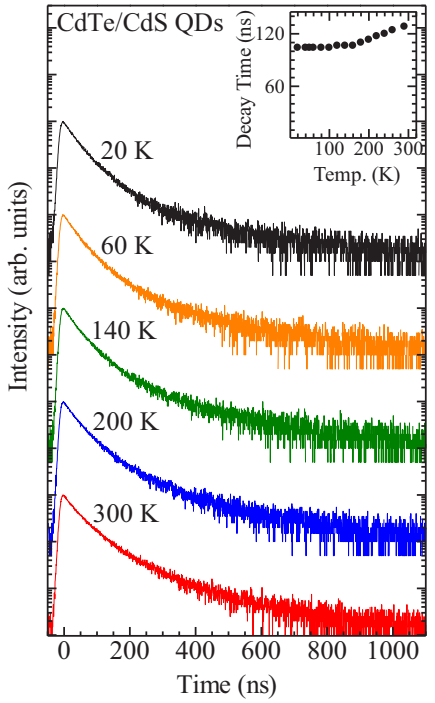

FIG. 7. PL decay profiles of CdTe/CdS QDs at 20, 60, 140, 200, and 300 K. The inset shows temperature dependence of PL decay time $\langle\tau_1\rangle$.

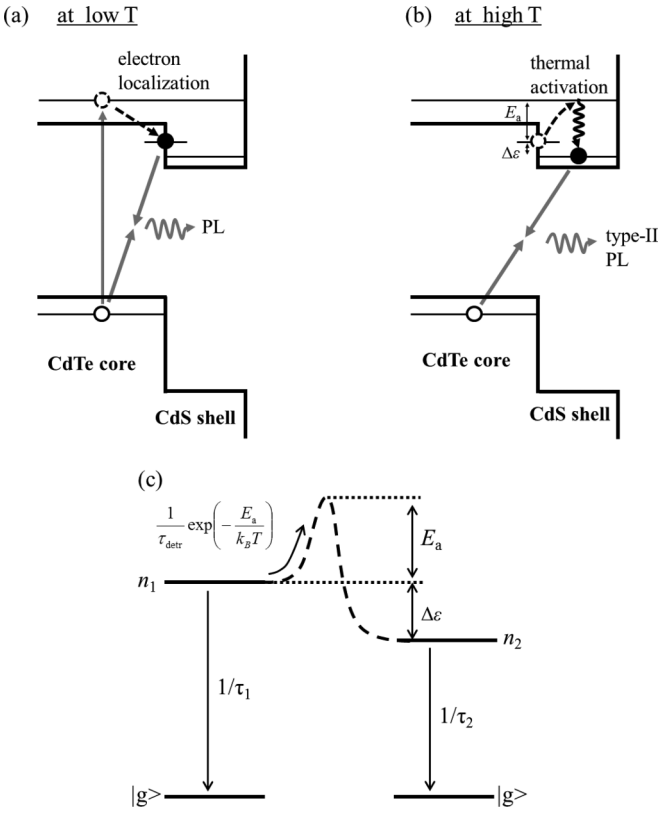

FIG. 8. Possible explanation model for the temperature dependence of $\langle\tau_1\rangle$. (a) At low temperature, localized-exciton state at the interface of core and shell mainly contributes to PL. (b) Thermal activation of localized excitons into the lower-lying type-II exciton state is accelerated with an increase in temperature. (c) Schematic energy diagram of used model showing the energy levels and the recombination and thermal activation channels.

both PL intensity and decay time. Although the influence of the nonradiative-decay rate is very small, as discussed in Fig. 5, the PL intensity decreases slightly with temperature. Nevertheless, $\langle\tau_1\rangle$ does not become shorter but longer at temperatures higher than 120 K. Thus, the temperature dependence of $\langle\tau_1\rangle$ cannot be explained by a simple two-level system comprising an excited state and a ground state, and we have to consider the contributions of at least two radiative states to the PL processes.

We discuss the origin of the unusual temperature dependence of $\langle\tau_1\rangle$ in conjunction with that of the Stokes shift. As a possible explanation (Fig. 8), we consider two emitting states: a higher-lying emitting state with a relatively fast decay time and a lower-lying emitting state with a relatively slow decay time. The state with a fast decay time mainly contributes to PL at low temperature [Figs. 8(a) and 8(c)]. Then, the thermal activation of excitons into the lower-lying emitting state with a slow decay time is accelerated with an increase in temperature [Figs. 8(b) and 8(c)]. Based on this model, we can expect that the contribution of the lower-lying state to PL increases with increased temperature, leading to prolongation of the decay time and increase in the Stokes shift. A decay time of $\langle\tau_1\rangle$ is ~130 ns at room temperature, which is much longer than that in CdSe and CdTe type-I QDs. Thus, we describe the lower-lying emitting state with a slow decay time as a type-II exciton state [Fig. 8(b)].

We consider a localized-exciton state at the interface between the core and the shell as the origin of the upper-lying emitting state with a fast decay time. In CdTe/CdS type-II QDs, after a photoexcitation an electron relaxes into a CdS shell, and a hole is confined to the CdTe core. Lattice mismatch between CdTe and CdS is 11% [47,48]. The strain induced by lattice mismatch would affect the relaxation and PL processes of excited carriers, especially at low temperatures. If electrons are localized to the interface of core/shell heterostructures before relaxing into the shell at low temperature [Fig. 8(a)], the overlap integral between the electron and the hole will become larger compared with that of a type-II exciton. Thus, the localized-exciton state has a shorter radiative-decay time. With an increase in temperature, the electron begins to relax into the shell by thermal-energy-assisted detrapping from the localized state, and the contribution of the type-II exciton state to the PL process becomes larger [Fig. 8(b)]. As a consequence, the observed decay time becomes larger with an increase in temperature above 120 K.

In order to quantitatively discuss the temperature dependence of the PL decay profiles, we have developed a simple phenomenological rate-equation model. Figure 8(c) shows the schematic energy diagram of the model used, showing the energy levels and the recombination and thermal-activation channels:

$$\frac{dn_1(t)}{dt} = -\frac{n_1(t)}{\tau_1} - \frac{n_1(t)}{\tau_{\text{detr}}}e^{-(E_a/k_BT)} + \frac{n_2(t)}{\tau_{\text{detr}}}e^{-[(E_a+\Delta\varepsilon)/k_BT]},$$
$$\frac{dn_2(t)}{dt} = -\frac{n_2(t)}{\tau_2} - \frac{n_2(t)}{\tau_{\text{detr}}}e^{-[(E_a+\Delta\varepsilon)/k_BT]} + \frac{n_1(t)}{\tau_{\text{detr}}}e^{-(E_a/k_BT)}, \quad (1)$$

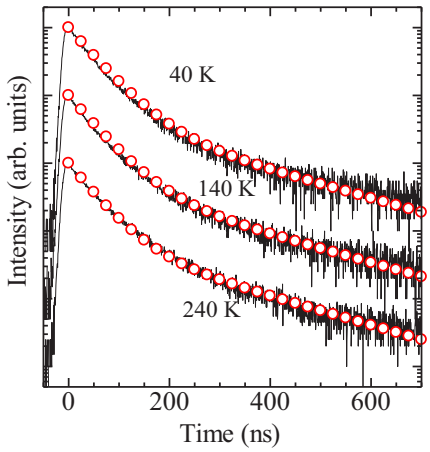

FIG. 9. Comparison of numerical solutions (open circles) of the rate-equation model with the measured PL decay profiles at 40, 140, and 240 K.

where $n_1(t)$ [$n_2(t)$] and $1/\tau_1$ ($1/\tau_2$) denote the population- and radiative-decay rates, respectively, of localized-exciton states (type-II exciton states). $e^{-(E_a/k_BT)}/\tau_{\rm detr}$ and $e^{-[(E_a+\Delta\varepsilon)/k_BT]}/\tau_{\rm detr}$ are the thermal-energy-assisted detrapping rate from the localized state and its reverse-process rate, respectively, where E_a is the thermal-activation energy and $\Delta\varepsilon$ represents the energy difference between localized-exciton and type-II exciton states. The detected PL intensity $I(t)$ is composed of a superposition of emission from the localized-exciton and type-II exciton states and is given by

$$I(t) \propto \frac{n_1(t)}{\tau_1} + \frac{n_2(t)}{\tau_2}. \tag{2}$$

In Fig. 9, numerical solutions of the rate-equation model are compared with the experimental results as functions of temperature. The experimental PL decay profiles can be well reproduced by the present model. The parameters were set to $\tau_1 = 50$ ns, $\tau_2 = 210$ ns, $\tau_{\rm detr} = 110$ ns, $E_a = 36$ meV, and $\Delta\varepsilon = 47$ meV, for which the best fitting of the experimental PL decay profiles was achieved. The decay time of $\tau_2 = 210$ ns is much longer than $\tau_1 = 50$ ns, indicating the smallness of the oscillator strength of the lower-lying emitting state. This result supports the appropriateness of the assumption that the origin of the lower-lying emitting state is the type-II exciton state. The activation energy of $E_a = 36$ meV may possibly correspond to localization energy of the electron [Fig. 8(a)].

Noteworthy observations to be made in the present study include the fact that the Stokes shift and observed PL decay time become larger with increased temperature. As discussed above, the findings are interpreted by considering thermal activation between two emitting localized-exciton and type-II exciton states. In Ref. [49], Wang *et al.* studied the temperature dependence of the PL intensity and PL decay profiles in CdTe/CdSe type-II QDs and reported that the radiative-decay time becomes longer with temperature. However, the experimentally observed decay profiles become shorter with an increase in temperature, reflecting the influence of the nonradiative-decay process; the PL intensity at room temperature is 13 times weaker than that at a low temperature of 20 K [49]. The authors extracted the temperature dependences of radiative- and nonradiative-decay times on the basis of a simple two-level system consisting of excited and ground states. On the contrary, in this work it is noted that the PL intensity at room temperature is ~80% of that at 20 K, meaning that the influence of the nonradiative-decay process is very small in the present CdTe/CdS QDs. Thus, the prolonged PL decay profiles at elevated temperature are experimentally observed.

Another important factor may be the smallness of the splitting energy ΔE between the bright-exciton and dark-exciton states in CdTe QDs. If ΔE is larger than a few meV, the radiative-decay time itself depends upon the temperature and becomes shorter with an increase in temperature, as often reported in CdSe QDs [40,41]. In such a case, it would be difficult to observe a small change in decay time originating from carrier localization and thermal-energy-assisted detrapping processes. Thus, two important features—the smallness of ΔE and the strong suppression of the nonradiative process—enable us to observe the effect of carrier localization at the interface of the core/shell heterojunction at low temperature and thermal-energy-assisted detrapping from the localized exciton to the type-II exciton states.

IV. CONCLUSION

The temperature dependence of the absorption and PL spectra, as well as the PL decay profiles of CdTe and CdTe/CdS type-II QDs, have been studied systematically. The Stokes shift in the CdTe/CdS QDs becomes larger with increasing temperature above 120 K, while it is independent of temperature in CdTe QDs. In CdTe QDs, PL decay time is almost constant above 70 K, because the splitting energy between the bright-exciton and dark-exciton states and the thermal-quenching effect is small. Conversely, the decay time in CdTe/CdS QDs exhibits characteristic temperature dependence. In the temperature region between 20 and 120 K, PL decay time is almost constant and becomes longer with an increase in temperature above 120 K. The localized-exciton state at the core/shell interface with a fast decay time mainly contributes to PL at low temperature. With an increase in temperature, the thermal activation of excitons into lower-lying type-II state with a slow decay time is accelerated. This thermal-energy-assisted detrapping from the localized-exciton to the type-II exciton states causes the increase of the Stokes shift and PL decay time at higher temperatures. The temperature dependences of the experimentally observed PL decay profiles are quantitatively reproduced by use of a simple phenomenological rate equation model.

[1] A. P. Alivisatos, Science **271**, 933 (1996).
[2] W. C. W. Chan and S. Nie, Science **281**, 2016 (1998).
[3] E. Kapon, D. M. Hwang, and R. Bhat, Phys. Rev. Lett. **63**, 430 (1989).

[4] L. T. Canham, Appl. Phys. Lett. **57**, 1046 (1990).
[5] Y. Arakawa and H. Sakaki, Appl. Phys. Lett. **40**, 939 (1982).
[6] R. L. Greene, K. K. Bajaj, and D. E. Phelps, Phys. Rev. B **29**, 1807 (1984).
[7] P. A. Schultz, K. Leung, and E. B. Stechel, Phys. Rev. B **59**, 733 (1999).
[8] P. W. Fry, I. E. Itskevich, D. J. Mowbray, M. S. Skolnick, J. J. Finley, J. A. Barker, E. P. O'Reilly, L. R. Wilson, I. A. Larkin, P. A. Maksym, M. Hopkinson, M. Al-Khafaji, J. P. R. David, A. G. Cullis, G. Hill, and J. C. Clark, Phys. Rev. Lett. **84**, 733 (2000).
[9] S. H. Xin, P. D. Wang, A. Yin, C. Kim, M. Dobrowolska, J. L. Merz, and J. K. Furdyna, Appl. Phys. Lett. **69**, 3884 (1996).
[10] M. Rabe, M. Lowisch, and F. Henneberger, J. Cryst. Growth **184–185**, 248 (1998).
[11] C. B. Murray, D. J. Noms, and M. G. Bawendi, J. Am. Chem. Soc. **115**, 8706 (1993).
[12] D. J. Norris, Al. L. Efros, M. Rosen, and M. G. Bawendi, Phys. Rev. B **53**, 16347 (1996).
[13] C. A. Smith, H. W. H. Lee, V. J. Leppert, and S. H. Risbud, Appl. Phys. Lett. **75**, 1688 (1999).
[14] H. S. Chen and S. J. J. Wang, Appl. Phys. Lett. **86**, 131905 (2005).
[15] L. Li, T. J. Daou, I. Texier, T. T. K. Chi, N. Q. Liem, and P. Reiss, Chem. Mater. **21**, 2422 (2009).
[16] T. Pons, E. Pic, N. Lequeux, E. Cassette, L. Bezdetnaya, F. Guillemin, F. Marchal, and B. Dubertret, ACS Nano **4**, 2531 (2010).
[17] J. Zhang, R. Xie, and W. Yang, Chem. Mater. **23**, 3357 (2011).
[18] J. M. Caruge, J. E. Halpert, V. Wood, V. Bulović, and M. G. Bawendi, Nat. Photonics **2**, 247 (2008).
[19] W. S. Song and H. Yang, Chem. Mater. **24**, 1961 (2012).
[20] J. K. Jaiswal, H. Mattoussi, J. M. Mauro, and S. M. Simon, Nat. Biotechnol. **21**, 47 (2002).
[21] S A. McDonald, G. Konstantatos, S. Zhang, P. W. Cyr, E. J. D. Klem, L. Levina, and E. H. Sargent, Nat. Mater. **4**, 138 (2005).
[22] P. K. Santra, P. V. Nair, K. G. Thomas, and P. V. Kamat, J. Phys. Chem. Lett. **4**, 722 (2013).
[23] M. Nirmal, D. J. Norris, M. Kuno, M. G. Bawendi, A. L. Efros, and M. Rosen, Phys. Rev. Lett. **75**, 3728 (1995).
[24] A. L. Efros, M. Rosen, M. Kuno, M. Nirmal, D. J. Norris, and M. Bawendi, Phys. Rev. B **54**, 4843 (1996).
[25] B. O. Dabbousi, J. Rodriguez-Viejo, F. V. Mikulec, J. R. Heine, H. Mattoussi, R. Ober, K. F. Jensen, and M. G. Bawendi, J. Phys. Chem. B **101**, 9463 (1997).
[26] V. V. Nikesh and S. Mahamuni, Semicond. Sci. Technol. **16**, 687 (2001).
[27] L. Li, A. Pandey, D. J. Werder, B. P. Khanal, J. M. Pietryga, and V. I. Klimov, J. Am. Chem. Soc. **133**, 1176 (2011).
[28] Y. Chen, T. Ji, and Z. Rosenzweig, Nano Lett. **3**, 581 (2003).
[29] A. V. Baranov, Y. P. Rakovich, J. F. Donegan, T. S. Perova, R. A. Moore, D. V. Talapin, A. L. Rogach, Y. Masumoto, and I. Nabiev, Phys. Rev. B **68**, 165306 (2003).
[30] S. Kim, B. Fisher, H. J. Eisler, and M. Bawendi, J. Am. Chem. Soc. **125**, 11466 (2003).
[31] V. I. Klimov, S. A. Ivanov, J. Nanda, M. Achermann, I. Bezel, J. A. McGuire, and A. Piryatinski, Nature (London) **447**, 441 (2007).
[32] Q. Zeng, X. Kong, Y. Sun, Y. Zhang, L. Tu, J. Zhao, and H. Zhang, J. Phys. Chem. C **112**, 8587 (2008).
[33] W. Zhang, G. Chen, J. Wang, B. Ye, and X. Zhong, Inorg. Chem. **48**, 9723 (2009).
[34] D. Zhao, Z. He, W. H. Chan, and M. M. F. Choi, J. Phys. Chem. C **113**, 1293 (2009).
[35] T. Watanabe, K. Takahashi, K. Shimura, H. B. Bu, H. D. Kim, and D. Kim, Bull. Chem. Soc. Jpn. **90**, 52 (2017).
[36] S. A. Ivanov, J. Nanda, A. Piryatinski, M. Achermann, L. P. Balet, I. V. Bezel, P. O. Anikeeva, S. Tretiak, and V. I. Klimov, J. Phys. Chem. B **108**, 10625 (2004).
[37] Y. P. Varshni, Physica **34**, 149 (1967).
[38] J. Camassel, D. Auvergne, H. Mathieu, R. Triboulet, and Y. Marfaing, Solid State Commun. **13**, 63 (1973).
[39] J. Jouglar, C. Hetroit, P. L. Vuillermoz, and R. Triboulet, J. Appl. Phys. **51**, 3171 (1980).
[40] S. A. Crooker, T. Barrick, J. A. Hollingsworth, and V. I. Klimov, Appl. Phys. Lett. **82**, 2793 (2003).
[41] C. de Mello Donegá, M. Bode, and A. Meijerink, Phys. Rev. B **74**, 085320 (2006).
[42] O. Schöps, N. L. Thomas, U. Woggon, and M. V. Artemyev, J. Phys. Chem. B **110**, 2074 (2006).
[43] J. H. Blokland, V. I. Claessen, F. J. P. Wijnen, E. Groeneveld, C. de Mello Donegá, D. Vanmaekelbergh, A. Meijerink, J. C. Maan, and P. C. M. Christianen, Phys. Rev. B **83**, 035304 (2011).
[44] T. J. Liptay and R. J. Ram, Appl. Phys. Lett. **89**, 223132 (2006).
[45] G. Morello, M. D. Giorgi, S. Kudera, L. Manna, R. Cingolani, and M. Anni, J. Phys. Chem. C **111**, 5846 (2007).
[46] T. J. Liptay, L. F. Marshall, P. S. Rao, R. J. Ram, and M. G. Bawendi, Phys. Rev. B **76**, 155314 (2007).
[47] A. M. Smith, A. M. Mohs, and S. Nie, Nat. Nanotechnol. **4**, 56 (2009).
[48] A. M. Smith and S. Nie, Acc. Chem. Res. **43**, 190 (2010).
[49] C. H. Wang, T. T. Chen, Y. F. Chen, M. L. Ho, C. W. Lai, and P. T. Chou, Nanotechnology **19**, 115702 (2008).